# Ferromagnetism in Topochemically Prepared Layered Perovskite $Li_{0.3}Ni_{0.85}La_2Ti_3O_{10}$

Doinita Neiner,[†,§] Leonard Spinu,[§,‡] Vladimir Golub,[⊥] and John B. Wiley*[,†,§]

*Department of Chemistry, Department of Physics, and Advanced Materials Research Institute, University of New Orleans, New Orleans, Louisiana 70148-2820, and Institute of Magnetism, National Academy of Sciences of Ukraine, 36-B Vernadsky Strasse, 0314 Kiev, Ukraine*

*Received July 26, 2005. Revised Manuscript Received November 9, 2005*

A nickel layer has been inserted between the perovskite blocks of triple-layer Ruddlesden−Popper titanate $Li_2La_2Ti_3O_{10}$ by ion exchange. The reaction takes place at low temperature (50−65 °C) in aqueous solution. Rietveld refinement of X-ray powder diffraction data indicates that $Li_{0.3}Ni_{0.85}La_2Ti_3O_{10}$ has Ni in a tetrahedral coordination. In terms of thermal stability, this material is a metastable phase, decomposing above 300 °C in both inert and oxidizing atmospheres. The magnetic data for $Li_{0.3}Ni_{0.85}La_2Ti_3O_{10}$ show Curie−Weiss behavior at high temperatures, with a magnetic moment in agreement with the presence of $Ni^{2+}$ ($S = 1$). At lower temperatures, two magnetic transitions take place, one at 23 K and one at 10 K. The transition at 23 K is ferromagnetic, and the one at 10 K is spin-glasslike. The magnetic entropy gained at the ferromagnetic transition (9.15 J/K) has been calculated from specific heat measurements at low temperatures, and is consistent with an $S = 1$ system. The observation of ferromagnetism is rare in nickel oxides, and this is discussed in terms of the composition and structure of this compound.

## Introduction

The reactivity of the A′ cations makes Ruddlesden−Popper (RP) compounds $A_2'[A_{n-1}B_nO_{3n+1}]$ (A′ is an alkali metal, A is an alkaline earth or rare earth metal, and B is a transition-metal cation) effective precursors to new low-temperature phases via topochemical routes. One of the most effective topotactic synthetic methods is the replacement of the A′ cations via an ion-exchange reaction. These reactions can take place in either aqueous medium, molten salts, or the solid state. In addition, monovalent and divalent ions can be exchanged. Monovalent ion exchange has led to $H_2La_2Ti_3O_{10}$ by an acidic aqueous-solution reaction.[1] Also, $Li_2La_2Ti_3O_{10}$ is a compound that has been obtained only by an ion-exchange reaction in a molten state, using $Na_2La_2Ti_3O_{10}$ and a large excess of $LiNO_3$.[2] In our group, we have shown that by using a two-step, low-temperature route (divalent ion exchange and then reductive intercalation), we can obtain mixed-valence compounds, such as $Na_{2-x+y}Ca_{x/2}La_2Ti_3O_{10}$, that exhibit semiconducting behavior.[3] Divalent ion exchange can also be performed, using transition-metal ions or cationic units. Through an aqueous-solution reaction using vanadyl sulfate hydrate and $K_2La_2Ti_3O_{10}$, Gopalakrishnan and co-workers showed that potassium ions could be replaced with vanadyl units.[4] Also, using a solid-state reaction, the RP compound $K_2La_2Ti_3O_{10}$, and BiOCl, the same authors obtained an Aurivillius phase $(BiO)La_2Ti_3O_{10}$.[4] In $Na_2La_2Ti_3O_{10}$, Hyeon and Byeon replaced sodium ions with transition-metal cations (Co, Cu, Zn) using a eutectic mixture of alkali-metal chlorides and transition-metal chlorides in sealed tubes;[5] by using an aqueous-solution reaction between nickel nitrate and $K_2Eu_2Ti_3O_{10}$, Schaak and Mallouk replaced potassium ions with nickel.[6] Herein, we describe an extension of such ion-exchange reactions in the triple-layered Ruddlesden−Popper series to obtain $Li_{0.3}Ni_{0.85}La_2Ti_3O_{10}$ by an aqueous-solution reaction. Also included are the synthesis, crystal structure, thermal behavior, and magnetic properties of this new compound. Especially interesting is the observation of ferromagnetism, an uncommon feature in nickel oxides.

## Experimental Section

**1. Synthesis.** $Na_2La_2Ti_3O_{10}$ was prepared by a solid-state reaction from $Na_2CO_3$, $La_2O_3$, and $TiO_2$ (all from Alfa Aesar, 99.99% purity). A 30% molar excess of $Na_2CO_3$ was used to compensate for the loss attributable to volatilization. The reagents were pressed into pellets, fired at 550 °C for 6 h, and then sintered at 1050 °C for 12 h.[2] After the reaction, we removed unreacted $Na_2CO_3$ by washing the solution with warm water; the sample was then rinsed with acetone, and was dried at 150 °C overnight. Phase purity for $Na_2La_2Ti_3O_{10}$ was confirmed by X-ray powder diffraction (XRD); the sample was indexed on a tetragonal unit cell with $a = 3.8352(7)$ Å and $c = 28.5737(7)$ Å, which is in agreement with the values reported in the literature.[2] Sodium was replaced with lithium by an ion-exchange reaction between $Na_2La_2Ti_3O_{10}$ and $LiNO_3$ in a 1:15 molar ratio for 2 days at 300 °C. Phase purity for $Li_2La_2$-

* To whom correspondence should be addressed. E-mail: jwiley@uno.edu.
† Department of Chemistry, University of New Orleans.
‡ Department of Physics, University of New Orleans.
§ Advanced Materials Research Institute, University of New Orleans.
⊥ National Academy of Sciences of Ukraine.

(1) Gopalakrishnan, J.; Uma, S.; Bhat, V. *Chem. Mater.* **1993**, *5*, 132.
(2) Toda, K.; Watanabe, J.; Sato, M. *Mater. Res. Bull.* **1996**, *31*, 1427.
(3) Lalena, J. N.; Cushing, B. L.; Falster, A. U.; Simmons, W. B., Jr.; Seip, C. T.; Carpenter, E. E.; O'Connor, C. J.; Wiley, J. B. *Inorg. Chem.* **1998**, *37*, 4484.
(4) Gopalakrishnan, J.; Sivakumar, T.; Ramesha, K.; Thangadurai, V.; Subanna, G. N. *J. Am. Chem. Soc.* **2000**, *122*, 6237.
(5) Hyeon, K.-A.; Byeon, S.-H. *Chem. Mater.* **1999**, *11*, 352.
(6) Schaak, R.; Mallouk, T. E. *J. Am. Chem. Soc.* **2000**, *122*, 2798.

10.1021/cm0516457 CCC: $33.50 
Published on Web 12/21/2005

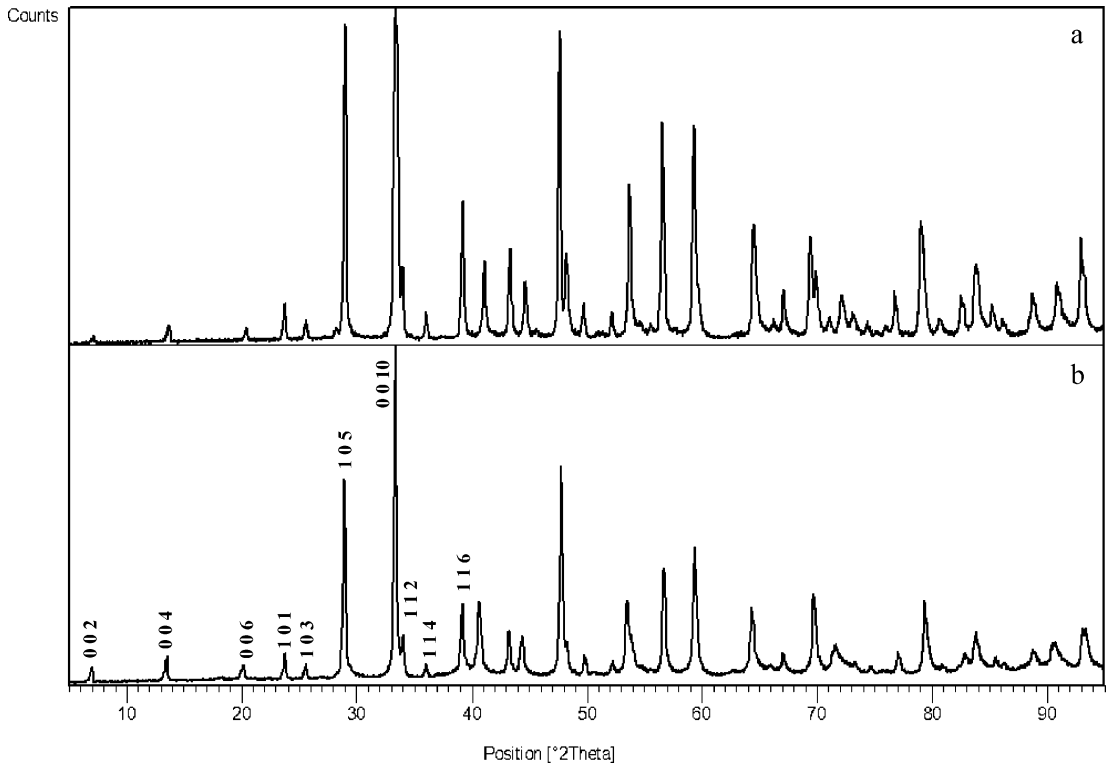


**Figure 1.** Comparison of the X-ray powder patterns for (a) $Li_2La_2Ti_3O_{10}$ and (b) $Li_{0.3}Ni_{0.85}La_2Ti_3O_{10}$.

$Ti_3O_{10}$ was verified by XRD. The powder pattern for this compound was refined on a tetragonal cell with $a = 3.8411(6)$ Å and $c = 26.5601(2)$ Å, which is in agreement with literature values for this material.[2]

$Li_{0.3}Ni_{0.85}La_2Ti_3O_{10}$ was prepared by an aqueous-solution reaction (150 mL of water) between $Li_2La_2Ti_3O_{10}$ and $NiCl_2$ in a 1:2 molar ratio at 50−65 °C under continuous stirring for 8 days. The reaction mixture was refreshed with a new nickel chloride solution after 4 days. The reaction can also take place if $Ni(NO_3)_2$ is used. The final product was washed with distilled water and acetone, and was dried at 100 °C overnight. $Li_{0.3}Ni_{0.85}La_2Ti_3O_{10}$ has a pale green color. Reactions between $NiCl_2$ and $A_2La_2Ti_3O_{10}$ (A = Na, K) were also investigated, but these did not show any evidence for ion exchange.

**2. Characterization.** Elemental analysis of Ti, Ni, and La was carried out by energy dispersive spectroscopy (EDS) on a series of individual crystallites using a JEOL (model JSM-5410) scanning electron microscope (SEM) equipped with an EDAX (DX-PRIME) microanalytical system. Lithium content was determined by inductively coupled plasma emission spectroscopy (ICP) analysis. The samples were dissolved in concentrated nitric acid. Standard solutions were prepared from Specpure Alfa Aesar 10 000 $\mu$g/mL for lithium. All the standards and samples were analyzed in a 5% $HNO_3$ solution (v/v). The composition of the final product corresponded to the general formula $Li_{0.30(1)}Ni_{0.85(2)}La_2Ti_{3.00(2)}O_{10}$.

X-ray powder diffraction studies were carried out on a Philips X'Pert System (Cu K$\alpha$ radiation, $\lambda = 1.5418$ Å) equipped with a graphite monochromator. Data were collected in a continuous scan mode between 5 and 95° 2$\theta$. The lattice parameters were refined using POLSQ.[7] Structural refinement was done by the Rietveld method with the GSAS package of programs.[8] The refined parameters include background, peak shape, cell, atom positions, scale factor, and thermal parameters. The $R$ factor ($R_p$), weighted $R$ factor ($wR_p$), and goodness of fit $\chi^2$ are defined as follows: $R_p = \sum[y_{io} - y_{ic}]/\sum y_{io}$, $wR_p = [\sum w_i(y_{io} - y_{ic})^2/\sum w_i(y_{io})^2]^{1/2}$, and $\chi^2 = [wR_p/R_{exp}]^2$, where $R_{exp} = [(N - P)/\sum w_i y_{io}^2]^{1/2}$, $y_{io}$ and $y_{ic}$ are the observed and calculated intensities, respectively, $w_i$ is the weighting factor, $N$ is the total number of observed intensities when the background is refined, and $P$ is the number of adjusted parameters.

**Table 1. Variation of Unit Cell Parameters and Volume for the Investigated Materials**

| compd | $a$ (Å) | $c$ (Å) | $V$ (Å$^3$) |
|---|---|---|---|
| $Li_2La_2Ti_3O_{10}$ | 3.8411(6) | 26.5601(2) | 391.8(6) |
| $Li_{0.3}Ni_{0.85}La_2Ti_3O_{10}$ | 3.8483(1) | 26.9871(2) | 399.6(6) |

Thermal behavior was studied on a Netzsch 404 S differential scanning calorimeter (DSC); measurements were performed in oxidizing and inert atmospheres between room temperature and 800 °C by heating samples at 10 °C/min in $O_2$ and Ar, respectively.

dc magnetic measurements (ZFC/FC and hysteresis loops) were performed on a Quantum Design MPMS-5S superconducting quantum interference device (SQUID) magnetometer between 2 and 300 K in magnetic fields of 100 and 10 000 Oe. Heat capacity and ac susceptibility were investigated using a Quantum Design PPMS between 5 and 300 K.

## Results

**1. Synthesis.** The ability of Ruddlesden−Popper compound $A_2La_2Ti_3O_{10}$ (A = Li, Na, K) to undergo ion exchange with nickel chloride has been investigated. Ion exchange occurred only in reactions with $Li_2La_2Ti_3O_{10}$ and not with the sodium or potassium analogues. The chemical analysis of the $Li_2La_2Ti_3O_{10}$ exchange product indicated a Li:Ni:La:Ti ratio of 0.30(1):0.85(2):2:3.00(2). The degree of exchange did not increase even when the molar ratio of nickel chloride to the perovskite, the reaction temperature, or reaction time was increased.

(7) Keszler, D. A.; Ibers, J. A. *Modified POLSQ*; Department of Chemistry, Northwestern University: Evanston, IL, 1983.
(8) Larson, A.; Von Dreele, R. B. *GSAS: Generalized Structure Analysis System*; Los Alamos National Laboratory: Los Alamos, NM, 1994.

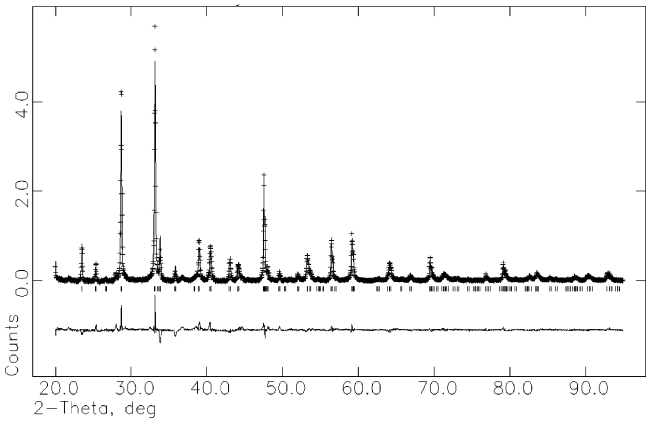


**Figure 2.** Calculated (solid line), experimental (crosses), and difference (lower line) plots for the Rietveld refinement of $Li_{0.3}Ni_{0.85}La_2Ti_3O_{10}$.

**Table 2. Crystallographic Data for $Li_{0.3}Ni_{0.85}La_2Ti_3O_{10}$**

| atom | site | *x* | *y* | *z* | g[a] | $U_{iso}$ (Å$^2$) |
|---|---|---|---|---|---|---|
| Ni | 4d | 0 | 0.5 | 0.25 | 0.425 | 0.011(7) |
| La | 4e | 0 | 0 | 0.4193(3) | 1.0 | 0.018(7) |
| Ti1 | 2a | 0 | 0 | 0 | 1.0 | 0.004(2) |
| Ti2 | 4e | 0 | 0 | 0.1560(8) | 1.0 | 0.035(1) |
| O1 | 4e | 0 | 0 | 0.07440(7) | 1.0 | 0.052(7) |
| O2 | 4c | 0 | 0.5 | 0 | 1.0 | 0.085(1) |
| O3 | 4e | 0 | 0 | 0.2334(1) | 1.0 | 0.023(5) |
| O4 | 8g | 0 | 0.5 | 0.1446(3) | 1.0 | 0.006(6) |

| param | value |
|---|---|
| space group | *I*4/*mmm* |
| *Z* | 2 |
| *a* (Å) | 3.8244(4) |
| *c* (Å) | 26.736(6) |
| *V* (Å$^3$) | 391.0(2) |
| $R_p$ (%) | 10.83 |
| $wR_p$ (%) | 14.52 |
| $\chi^2$ (%) | 3.11 |

[a] *g* = occupancy.

**Table 3. Bond Lengths (Å) and Angles (deg) for $Li_{0.3}Ni_{0.85}La_2Ti_3O_{10}$**

| | |
|---|---|
| Ni−O3 (×4) | 1.963(1) |
| Ti1−O1 (×2) | 1.989(4) |
| Ti1−O2 (×4) | 1.912(2) |
| Ti2−O1 (×1) | 2.183(6) |
| Ti2−O3 (×1) | 2.067(4) |
| Ti2−O4 (×4) | 1.936(5) |
| La−O1 (×4) | 2.709(4) |
| La−O2 (×4) | 2.882(3) |
| La−O4 (×4) | 2.565(5) |
| O3−Ni−O3 | 153.880(1) |
| O3−Ni−O3 | 92.927(1) |

**2. Structure.** Ion exchange between $Li_2La_2Ti_3O_{10}$ and $Ni^{2+}$(aq) takes place in a topotactic manner. In Figure 1, the XRD powder patterns for $Li_2La_2Ti_3O_{10}$ and $Li_{0.3}Ni_{0.85}La_2Ti_3O_{10}$ are presented. The ion-exchanged material was indexed on a tetragonal lattice with the cell parameters listed in Table 1. For $Li_{0.3}Ni_{0.85}La_2Ti_3O_{10}$, a Rietveld refinement was carried out. The observed, calculated, and difference plots are shown in Figure 2. The atomic positions and bond lengths and angles are presented in Tables 2 and 3, respectively. Lithium atoms were not included in the refinement.

**3. Thermal Behavior.** Differential scanning calorimetry for $Li_{0.3}Ni_{0.85}La_2Ti_3O_{10}$ in both oxidizing and inert atmospheres shows that this compound is a metastable phase that undergoes an exothermic transition around 300 °C. The DSC curves for $Li_{0.3}Ni_{0.85}La_2Ti_3O_{10}$ in inert and oxidizing atmospheres are presented in Figure 3. The XRD patterns after

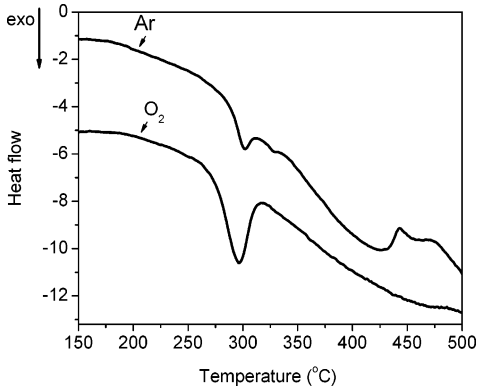


**Figure 3.** DSC curves in argon and oxygen for $Li_{0.3}Ni_{0.85}La_2Ti_3O_{10}$.

DSC at 200, 400, and 800 °C are shown in Figure 4. The XRD patterns after DSC show that at 400 °C, NiO starts forming, and at 800 °C, NiO constitutes the predominant phase. Mixed with the NiO is a defective perovskite phase, most likely $La_2Ti_3O_9$.[9]

**4. Magnetic Behavior and Heat Capacity.** The magnetic susceptibility as a function of temperature in 100 and 10 000 Oe fields, the linear fit of the reciprocal susceptibility vs temperature, and the hysteresis loops at 5, 20, and 40 K are shown in Figure 5a−d. From the linear fit of the 100 Oe data, we calculated a magnetic moment for $Li_{0.3}Ni_{0.85}La_2Ti_3O_{10}$ of $\mu = 2.97\ \mu_B$ and a Weiss constant of 5 K. The magnetic moment is in agreement with other values reported in the literature for a $d^8$ system in a tetrahedral ligand field.[10] From the variation of the magnetic moment as a function of temperature and from the positive Weiss constant, we determined that the transition at 23 K appears to be ferromagnetic. The magnetic behavior of this compound changes when the dc-applied magnetic field is 10 000 Oe. Under these conditions, the ZFC/FC curves split at the same temperature, but the transitions are broadened by the applied magnetic field. Figure 5d shows the presence of a hysteresis feature below both the first and second transitions; above these two transitions (40 K), the hysteresis is no longer observed.

Heat capacity measurements on $Li_{0.3}Ni_{0.85}La_2Ti_3O_{10}$ and $Li_2La_2Ti_3O_{10}$ were performed between 5 K and room temperature. Heat capacity data from 5 to 100 K are presented in Figure 6. $Li_{0.3}Ni_{0.85}La_2Ti_3O_{10}$ shows an inflection point at 23 K, indicative of a disorder−order transition. This transition can be correlated with the ferromagnetic transition seen in the dc magnetic data.

To extract the magnetic component of the heat capacity, we used the correspondent states law.[10] The nonmagnetic equivalent used in this case was the parent compound, $Li_2La_2Ti_3O_{10}$, where the heat capacity for the Li compound provides the lattice heat capacity for $Li_{0.3}Ni_{0.85}La_2Ti_3O_{10}$. The lattice component of the specific heat was then subtracted, and the resulting specific heat is shown in Figure 7. The magnetic entropy gained at the transition was calculated by integrating the area under the $C_p/T$ vs $T$ curve (Figure 7), and is consistent with an $S = 1$ magnetic system.[10]

$$S = \int (C_p/T)\, dT = R \ln(2S + 1) = 9.15\ \text{J mol}^{-1}\ \text{K}^{-1}$$

The heat capacity was also measured in the presence of a

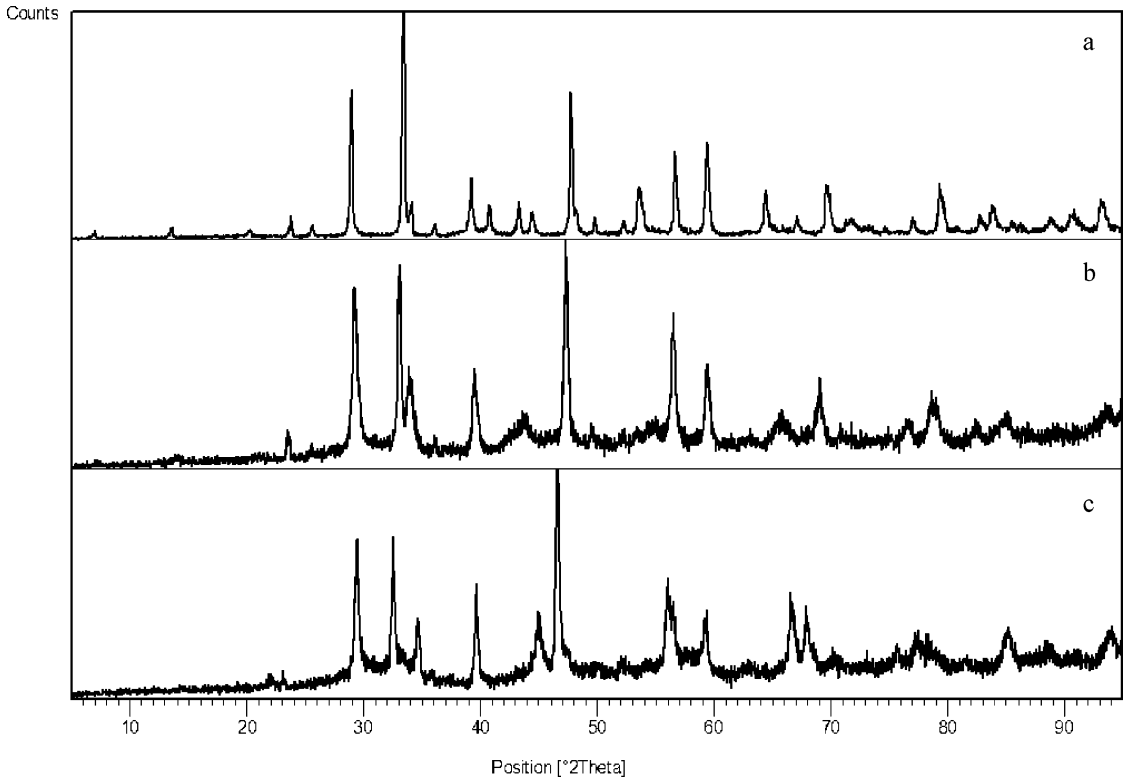


**Figure 4.** XRD for $Li_{0.3}Ni_{0.85}La_2Ti_3O_{10}$ after DSC in Ar at (a) 200, (b) 400, and (c) 800 °C.

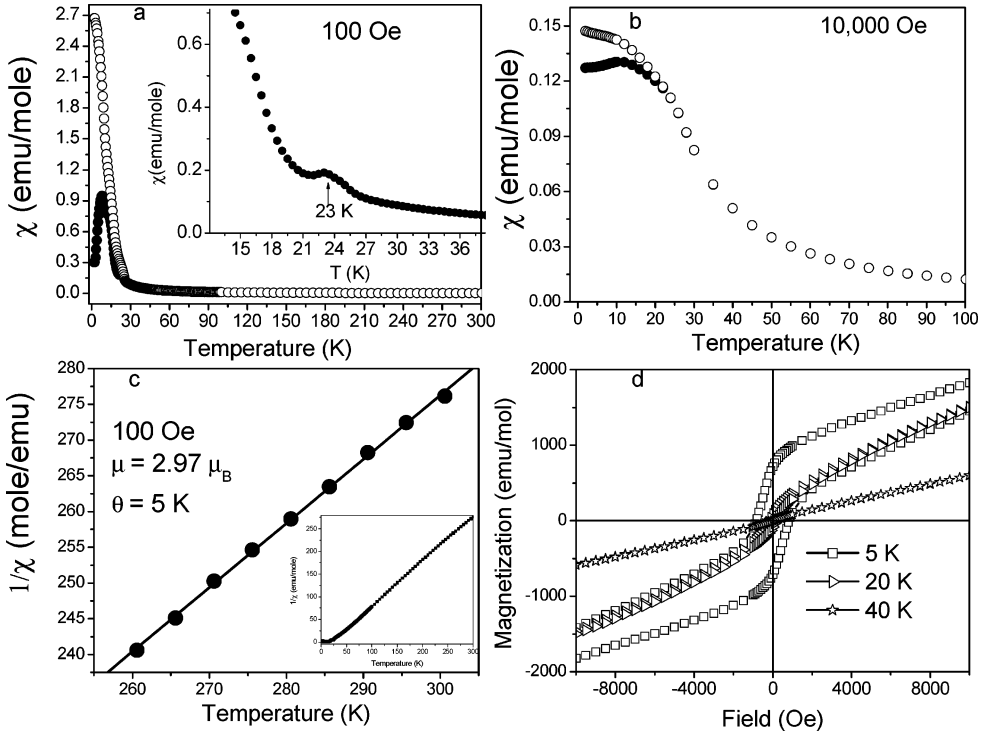


**Figure 5.** Magnetic behavior of $Li_{0.3}Ni_{0.85}La_2Ti_3O_{10}$. (a) Magnetic susceptibility vs *T* in a 100 Oe field (inset emphasizes the transition at 23 K), ZFC is shown as filled circles and FC as open circles. (b) Magnetic susceptibility vs *T* in a 10 000 Oe field. (c) Reciprocal susceptibility vs *T* along with the linear fit for the 100 Oe data. Inset presents the reciprocal susceptibility data for 2−300 K. (d) Hysteresis loops at 5, 20, and 40 K.

magnetic field of 10 000 Oe. Under these conditions, the transition shifts to higher temperatures and broadens (Figure 8). The shift to higher temperatures confirms the ferromagnetic nature of this transition.[11]

In Figures 9 and 10, the ac susceptibility measurements are presented. It can be seen from these figures that the transitions are present in both the real and imaginary components of the susceptibility. In addition, the transition

(9) Gopalakrishnan, J.; Bhat, V. *Inorg. Chem.* **1987**, *26*, 4301.
(10) Carlin, R. L. *Magnetochemistry*; Springer-Verlag: New York, 1986.
(11) Pecharsky, V. K.; Gschneidner, K. A., Jr.; Fort, D. *Phys. Rev. B* **1993**, *47*, 5063.

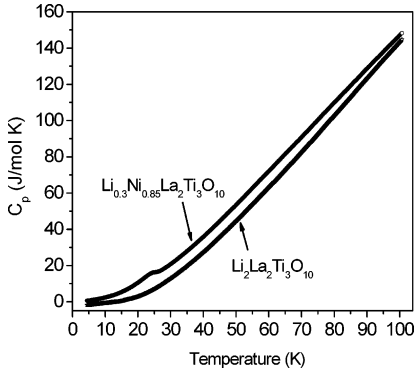


**Figure 6.** Heat capacity for $Li_2La_2Ti_3O_{10}$ and $Li_{0.3}Ni_{0.85}La_2Ti_3O_{10}$.

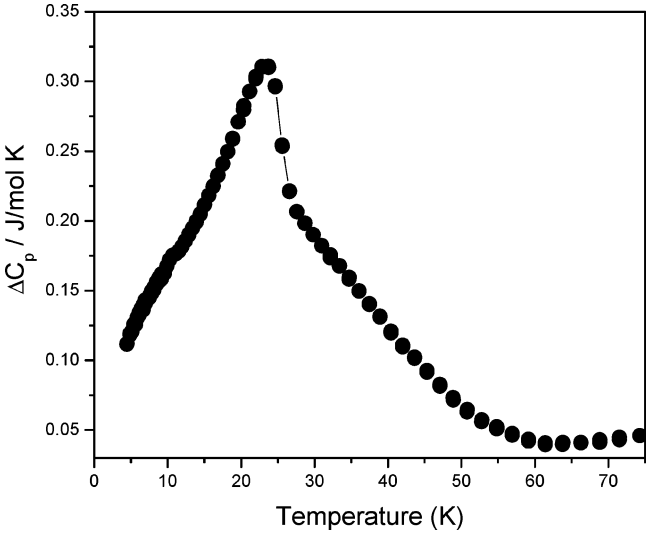


**Figure 7.** Magnetic contribution to the specific heat of $Li_{0.3}Ni_{0.85}La_2Ti_3O_{10}$.

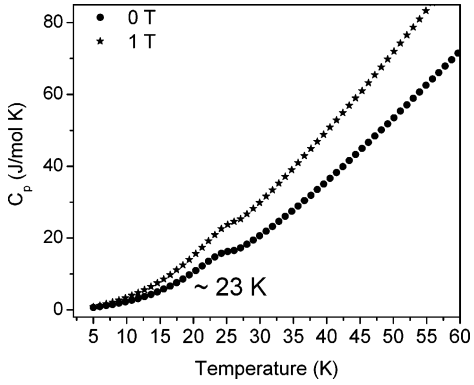


**Figure 8.** Heat capacity data for $Li_{0.3}Ni_{0.85}La_2Ti_3O_{10}$ at 0 and 1 T.

at 10 K is strongly frequency-dependent; it shifts to higher temperature as the frequency is increased. This is a characteristic of spin glasses and ferromagnets.[12−17] In the low-frequency limit of an ac measurement, spin glasses shift downward in temperature with decreasing applied frequency, whereas for ferromagnets and antiferromagnets, higher frequencies are needed.[22] In strong dc magnetic fields, the transition at 10 K shifts toward the high-temperature transition at 23 K. This behavior has been observed in spin glasses.[12,17]

## Discussion

The composition of the ion-exchanged product corresponds to the formula $Li_{0.30(1)}Ni_{0.85(1)}La_{2.00}Ti_{3.00(2)}O_{10}$. A complete exchange leading to Ni:La:Ti = 1:2:3 was not observed, even when the reaction conditions were varied. This has been observed in other layered systems, and has been attributed to the trapping of some alkali-metal cations between the perovskite blocks.[18] The structure of $Li_{0.30(1)}Ni_{0.85(2)}La_2Ti_3O_{10}$ is comparable to that of $Li_2La_2Ti_3O_{10}$ in that the $[La_2Ti_3O_{10}]$ layers have been maintained upon ion exchange. Although Ni occupies 42.5% of the sites, the unit cell size of $Li_{0.30(1)}Ni_{0.85(2)}La_2Ti_3O_{10}$ is expanded compared to that of $Li_2La_2Ti_3O_{10}$. Therefore, the trapping of lithium ions between the perovskite sheets does not occur, because of a reduction in the interlayer space.[18] The tetrahedral arrangement of the Ni between the perovskite layers, however, may act to suppress the extent of ion exchange beyond 70% by blocking lithium ion conduction pathways.

The thermal behavior of this compound exhibits an exothermic transition in both inert and oxidizing atmospheres. The XRD after DSC shows that, although the layered structure is maintained at 400 °C, there is a significant loss in crystallinity. By 800 °C, the layered structure is destroyed. This is presumably the reason this compound could not be prepared at 500 °C, because once it forms it decomposes.[5] The decomposition products are NiO and $La_2Ti_3O_9$. This is consistent with the metastability observed in other ion-exchanged layered perovskites.[5] $CuLa_2Ti_3O_{10}$ exhibits a similar behavior; its crystallinity degrades when heated in Ar at elevated temperatures, and it decomposes above 750 °C.[5] In addition, it demonstrates that $Li_{0.3}Ni_{0.85}La_2Ti_3O_{10}$ could not be obtained by traditional high-temperature synthetic methods, as it is not stable under these conditions.

$Li_{0.3}Ni_{0.85}La_2Ti_3O_{10}$ has unique magnetic behavior. In a small magnetic field of 100 Oe, the ZFC/FC curves split below 30 K. This is consistent with the magnetic ordering of nickel ions below this temperature. This behavior has been seen in both long-range magnetically ordered systems (ferromagnetic and ferrimagnetic) and spin glasses.[10,12−17] Below 30 K, two magnetic transitions occur, one at 23 K and one at 10 K. The magnetic moment calculated from the linear fit of the reciprocal susceptibility vs temperature (2.97 $\mu_B$) is consistent with an $S = 1$ magnetic system.[10] The fit also gives a positive Weiss constant, which suggests ferromagnetic interactions. In higher fields of 10 000 Oe, the

(12) Moorjani, K.; Coey, J. M. D. *Magnetic Glasses*; Elsevier: New York, 1984.
(13) Rayaprol, S.; Sengupta, K.; Sampathkumaran, E. V. *Phys. Rev. B* **2003**, *67*, 180404(R).
(14) Kaczorowski, D.; Noël, H. *J. Phys.: Condens. Matter* **1993**, *5*, 9185.
(15) Greedan, J. E. *J. Mater. Chem.* **2001**, *11*, 37.
(16) Matsuhira, K.; Hinatsu, Y.; Tenya, K.; Sakakibara, T. *J. Phys.: Condens. Matter* **2000**, *12*, L694.
(17) Rayaprol, S.; Sengupta, K.; Sampathkumaran, E. V. *Phys. Rev. B* **2003**, *67*, 180404(R).
(18) McIntyre, R. A.; Falster, A. U.; Li, S.; Simmons, W. B.; O'Connor, C. J.; Wiley, J. B. *J. Am. Chem. Soc.* **1998**, *120*, 217.
(19) Rao, C. N. R.; Paul, G.; Choudhury, A.; Sampathkumaran, E. V.; Raychaudhuri, A. K.; Ramasesha, S.; Rudra, I. *Phys. Rev. B* **2003**, *67*, 134425.
(20) Fisher, M. E. *Philos. Mag.* **1962**, *7*, 1731.
(21) Blasco, J.; Garcia, J.; Sanchez, M. C.; Larrea, A.; Campo, J.; Subias, G. *J. Phys.: Condens. Matter* **2001**, *13*, L729.
(22) Mydosh, J. A. *Spin Glasses, An Experimental Introduction*; Taylor & Francis: London, 1993.

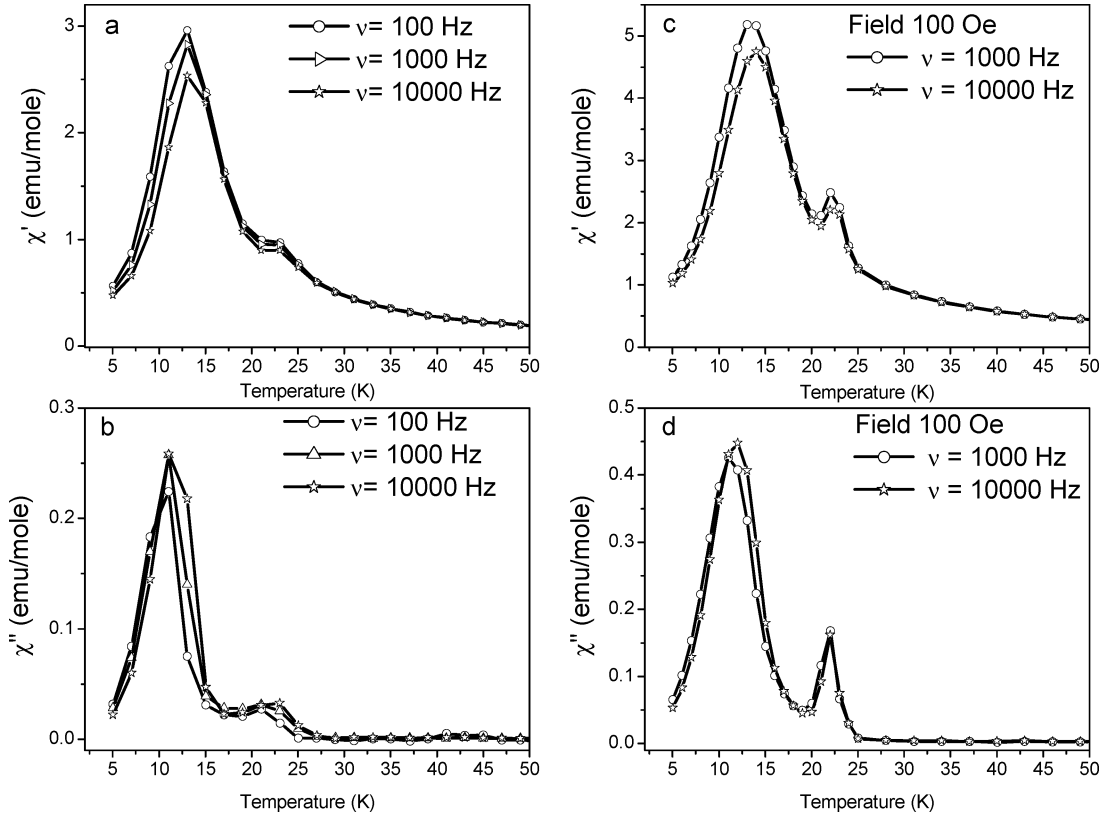


**Figure 9.** ac susceptibility for $Li_{0.3}Ni_{0.85}La_2Ti_3O_{10}$ at 100, 1000, and 10 000 Hz for real and imaginary components in the absence and presence of a dc magnetic field: (a) real component in the absence of a field, (b) imaginary component in the absence of a field, (c) real component in a 100 Oe dc field, and (d) imaginary component in a 100 Oe dc field.

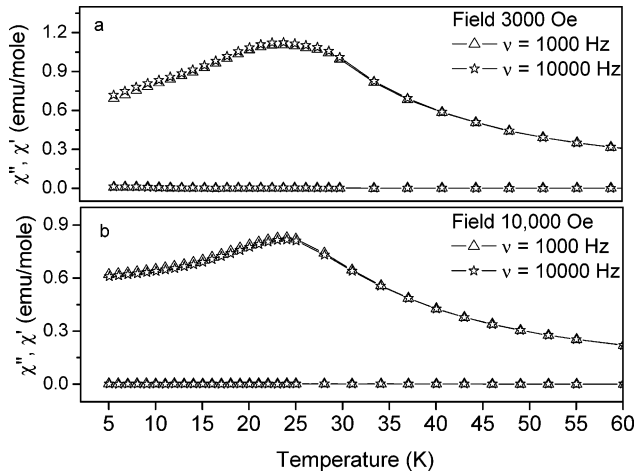


**Figure 10.** In-field ac susceptibility for $Li_{0.3}Ni_{0.85}La_2Ti_3O_{10}$ in high magnetic fields of (a) 3000 and (b) 10 000 Oe. The frequencies used are 1000 and 10 000 Hz.

magnetic behavior of $Li_{0.3}Ni_{0.85}La_2Ti_3O_{10}$ changes. The ZFC/FC curves split in the same temperature range as that in the low field (100 Oe); however, there is not a clear transition at 10 K, and the transition at 23 K broadens. Below this transition temperature (23 K), hysteretic behavior is observed at 20 and 5 K. The small saturation moment at 5 K, $M_s \approx 0.2\ \mu_B$/Ni (Figure 5d), compared to the high degree of spin ordering deduced from the entropy change at $T_c$, could be correlated to the presence of a glassy as opposed to a ferromagnetic one. An alternative reason for the small saturation magnetization is a very long relaxation time or weak ferromagnetism. Heat capacity data are consistent with an order−disorder transition at 23 K. In-field heat capacity data confirm the ferromagnetic origin of this transition, because with the applied field, the transition shifts to higher temperatures.[11] In addition, the magnetic entropy gained at the transition is consistent with an $S = 1$ system.[10] Furthermore, it can be seen from Figure 7 that there is a tail for the $C$ vs $T$ curve for the magnetic specific heat. This tail can be attributed to the Schottky anomaly because of nickel ion anisotropy.[10,12] Ferromagnetism in nickel oxides is quite rare, although it is not uncommon for Ni ions to arrange ferromagnetically. It is the structure of $Li_{0.030(1)}Ni_{(0.85(1)}La_{2.00}$-$Ti_{3.00(2)}O_{10}$ that makes a ferromagnetic arrangement possible in this compound. In an ideal 100% occupancy on the Ni site, ferromagnetism would probably not occur, because the Ni−O−Ni arrangement would facilitate a superexchange mechanism, giving an antiferromagnetic state. The occupancy on the Ni site is 42.5%, and if one removes every other nickel from the above-mentioned arrangement in a symmetric manner, then the nickel ions would be ferromagnetically arranged. If one removes the nickel ions asymmetrically, those Ni ions that do not have a Ni closest neighbor will be ferromagnetically arranged, whereas those that do will be antiferromagnetic. Therefore, the overall state will be ferromagnetic and frustrated. In addition, nickel ions ($d^8$) in the present compound are in a tetrahedral environment ($e^4t_2^4$), and none of the Ni−O3−Ni bond angles (see Table 3) is going to facilitate a strong superexchange antiferromagnetic interaction (which is strongest when the angle is 180° and weakest when the angle is 90°). Furthermore, disorder conceivably plays a very big role in that only 42.5% of the

nickel sites are filled. This is why, as will be discussed below, this compound has a high degree of frustration in its magnetic interactions.

For the 10 K transition, ac susceptibility measurements have been used to investigate the possibility of a spin-glasslike behavior. Because spin glasses are amorphous magnetic systems, ac susceptibility data are very useful for them, as their freezing point cannot be obtained from heat capacity measurements.[10,12] Also, ac data can help distinguish between ferromagnetic and antiferromagnetic types of ordering, because antiferromagnets lack a signal in the imaginary part of the ac susceptibility.[12] Because both transitions are present in the real as well as the imaginary part of the ac susceptibility, an antiferromagnetic order can be ruled out.[12,20−23] This is a characteristic of both spin glasses and ferromagnets.[12,22] It is generally difficult to distinguish between a ferromagnetic and a spin-glass transition, because they are so much alike. Both spin glasses and ferromagnets are characterized by ZFC/FC splitting, hysteresis loops, and frequency-dependent ac susceptibilities.[12,20−23] There are subtle differences, though. A sharp peak appears at the freezing point in spin glasses, whereas a sharp peak appears in ferromagnets at the Curie point. In contrast with ferromagnetic transitions, the spin-glass transition can be rounded by even small magnetic fields.[12−17] A strong frequency dependence of the transition at 10 K suggests that this transition is spin-glasslike.[22] Also, this transition shifts downward with decreasing applied frequency.[22] This behavior indicates that $Li_{0.3}Ni_{0.85}La_2Ti_3O_{10}$ is not a canonical spin glass but rather a spin-glasslike material.[22] Moreover, the transition at 23 K is frequency independent in the low-frequency regime, which confirms once more its ferromagnetic origin. As shown in Figures 9c,d and 10, small dc fields round the 10 K transition. The in-field ac susceptibility shows that the transition at 10 K is first rounded in small fields (Figure 9c,d), and completely shifts (Figure 10) in higher fields of 3 and 10 kOe. Also, the frequency dependence in the zero field disappears in 3 and 10 kOe fields, which confirms the spin-glasslike behavior.[19] It is very difficult to rule out another order−disorder transition on the basis of our specific heat data, as our measurements were performed between 5 and 300 K. It has been seen that the specific heat transition temperature can be displaced lower in temperature by as much as 10 K compared to that of the ZFC/FC data.[20] Therefore, although we cannot rule out another order−disorder transition on the basis of our specific heat data, ac susceptibility measurements enable us to reveal the spin-glasslike nature of the transition at 10 K.

Considering the crystal structure of $Li_{0.3}Ni_{0.85}La_2Ti_3O_{10}$, we can easily rationalize such magnetic behavior. When we replaced lithium (1+) with nickel (2+) only, the occupancy on the lithium site reduces to 42.5% to maintain the charge balance. The basic requirements for a glass state are the existence of disorder and frustration.[12,22] It is reasonable to assume that a structure having 42.5% occupancy for the magnetic ion site ($Ni^{2+}$) constitutes a disordered structure. Presumably, in such a disordered structure, frustration can occur whenever a nickel is missing. If one nickel is missing in such an arrangement, then the nearest-neighbor interactions will be frustrated. Thus, the spin-glass transition comes from an unsatisfied arrangement of the magnetic ions.

From this characterization, we can then put forward a magnetic phase diagram for $Li_{0.3}Ni_{0.85}La_2Ti_3O_{10}$. In the region 30−300 K, the compound shows paramagnetic behavior, followed by a ferromagnetic region 10−30 K, and spin-glasslike behavior below 10 K. Because the spin glass comes from a ferromagnetic state instead of a paramagnetic one, it can be classified as a reentrant spin glass.[12,20−23]

**Acknowledgment.** This material is based upon work supported by the National Science Foundation under Grant 0309972. Also, we gratefully acknowledge Prof. Charles O'Connor for helpful discussions.

CM0516457

(23) Cardoso, C. A.; Aranjo-Moreira, F. M.; Awana, V. S. P.; Takayama-Muromachi, E.; de Lima, O. F.; Yamauchi, H.; Karppinen, M. *Phys. Rev. B* **2003**, *67*, 020407(R).
(24) Paulus, W.; Cousson, A.; Dhalenne, G.; Berthon, J.; Revcolevschi, A.; Hosoya, S.; Treutmann, W.; Heger, G.; Le Toquin, R. *Solid State Sci.* **2002**, *4*, 565.
(25) Okajima, Y.; Kohn, K.; Siiratori, K. *J. Magn. Magn. Mater.* **1995**, *140−144*, 2149.
(26) Lewis, M. J.; Gaulin, B. D.; Filion, L.; Kallin, C.; Dabkowska, H. A.; Qiu, Y. *Phys. Rev. B* **2005**, *72*, 014408.